Thermomechanical and Ultrasonic Properties of High-Modulus Aromatic Polyamide Fibers

Tadaoki Ii, Kohji Tashiro, Masamichi Kobayashi,* and Hiroyuki Tadokoro

Department of Macromolecular Science, Faculty of Science, Osaka University, Toyonaka, Osaka 560, Japan. *Received February 18, 1986*

ABSTRACT: Bulk properties of highly oriented poly(*p*-benzamide) (PBA) and poly(*p*-phenyleneterephthalamide) (PPTA) have been investigated by thermomechanical analysis and ultrasonic measurement under the application of tensile stresses along the fiber direction, together with the thermogravimetry. In the temperature range 320–410 K, as-received samples have exhibited a dehydration phenomenon accompanied with a slight and irreversible increase in the fiber length, a transient slowing down of the increase in sonic compliance, and a dispersion of the sound attenuation constant. All these phenomena have been explained on the basis of some relaxational motion of the chains accommodated in the hydrated noncrystalline part. In the range 170–630 K, annealed samples have shown the following reversible phenomena: (1) a smooth and negative thermal expansion ($(-7 \text{ to } -11) \times 10^{-6}$ K^{-1} for PBA and $(-6 \text{ to } -9) \times 10^{-6}$ K^{-1} for PPTA); (2) an increase in sonic compliance (50% for PBA and 70% for PPTA); (3) a negative stress dependence of sonic compliance, $\partial J_s/\partial\sigma < 0$; and (4) $-\partial J_s/\partial\sigma$ becoming higher as temperature rises. J_s is the sonic compliance, and σ is the tensile stress. Phenomena 1–4 have been considered as a direct reflection of the mechanical and thermal behavior of the extended molecular chain characteristic of these polymer fibers and interpreted in terms of chain contraction which is due to the molecular motion perpendicular to the chain direction induced by thermal agitation.

Introduction

Poly(*p*-benzamide) (PBA) and poly(*p*-phenyleneterephthalamide) (PPTA) are well-known as rigid-rod polymers from which ultra-high-modulus fibers can be manufactured.[1-6] Their chains are composed of an alternate combination of amide and phenylene groups, and the internal rotations around the N–C_6H_4 and C–C_6H_4 bonds have much higher potential barriers than those around the skeletal single bonds in the usual flexible chain polymers.[1,2,7,8] Because of their rigidity, these polymers take extended chain conformation with a long distance order even in dilute solutions.[1,9-12] They also exhibit a liquid crystal phase in some concentrated solutions,[1-4,13-15] from which highly oriented and highly crystalline fibers can be spun.[1-6] In the crystal lattices of these fibers, the molecular chains take fully extended forms as below.[16-18]

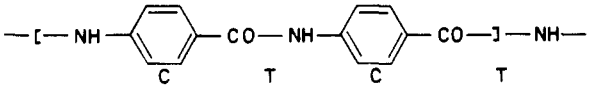

PBA

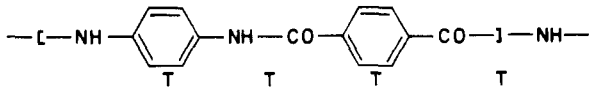

PPTA

Here N–C_6H_4–C and so on are assumed to be virtual bonds.[19] It has been considered that even in the noncrystalline part the chains still assume almost extended molecular conformations and are arrayed in parallel with poor lateral order (so-called paracrystalline structure).[18,20-22]

For these characteristic polymers, the microscopic moduli have been evaluated, the lattice or crystalline modulius by x-ray method[20,22-25] and the theoretical modulus on the basis of the extended structures.[26-28] On the other hand, the macroscopic modulus has been reported by many investigators, and the observed values for highly oriented PBA and PPTA fibers have reached nearly a half of the corresponding microscopic values. In the case of the usual crystalline polymers consisting of flexible chains, on the contrary, even for highly oriented states, the macroscopic properties such as elastic modulus and thermal expansibility are considerably modified from the microscopic properties of the crystalline part by the interactions with coexisting folding and amorphous parts.[29-32] Therefore, a close coincidence of the value between the macroscopic and microscopic moduli in PBA and PPTA fibers suggests the above-described morphological feature of these fibers from the mechanical point of view (refer to Tables I and II). The detailed investigation of the macroscopic properties of these fibers may be useful not only for understanding their characteristic properties but also for finding some unknown behavior of the fully extended chain. Such information will be applicable to research into inherent properties of the crystalline part of the usual flexible polymers.

Table I
Comparison of Moduli for PBA

Experimental Moduli, GPa			
	present study[a]		
	as-received	annealed	Slutsker et al.[25]
sonic	175	180	167
lattice			182

Theoretical Moduli, GPa			
confmn	Fielding-Russell[26]	Tadokoro et al.[28]	Perepelkin et al.[27]
trans	200	238	232
cis		163	178

[a] Moduli at room temperature measured for as-received and annealed PRD 49 under $\sigma = 0.109$ GPa.

In the present paper, we will describe the experimental results of thermomechanical analysis (TMA), ultrasonic measurement, and thermogravimetry (TG) and discuss both the irreversible phenomena observed for as-received samples and the reversible phenomena observed for annealed ones. Fortunately, these fibers show excellent heat stability and high tensile strength, making it possible to perform the above-mentioned measurements in wide ranges of temperature and stress.

Experimental Section

Materials. Three types of high-modulus fibers produced by Du pont were examined, namely PRD 49 (Type I) for PBA and Kevlar 49[33] and fiber B for PPTA. These sample fibers were confirmed to have the chemical structures of PBA and PPTA, respectively, on the basis of Raman and infrared spectra, the vibrational analysis of which will be reported elsewhere.[34] Densities of these fibers measured by the submerged cantilever method

0024-9297/86/2219-1809$01.50/0

Table II
Comparison of Moduli for PPTA

Experimental Moduli, GPa

	present study[a]					
	as-received	annealed	Slutsker et al.[25]	Northolt and Van Aartsen[22]	Gaymans et al.[24]	Kaji and Sakurada[23]
sonic	139	139	120	103		
lattice			182	112	200	153

Theoretical Moduli, GPa

confmn	Fielding-Russell[26]	Tadokoro et al.[28]	Perepelkin et al.[27]
trans	200	182	232
cis			178

[a] Moduli at room temperature measured for as-received and annealed Kevlar 49 under σ = 0.114 GPa.

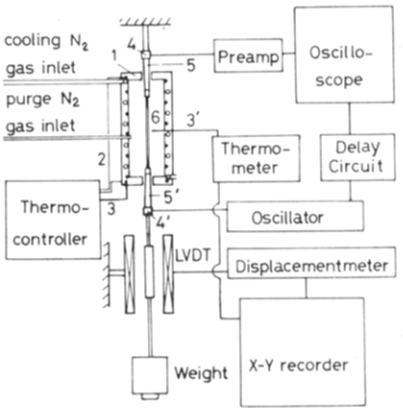

Figure 1. Schematic diagram of thermomechanical and ultrasonic measurement system: (1) thermocontrolled furnace; (2) heater; (3), (3′) thermocouple; (4), (4′) piezoelectric transducer; (5), (5′) fused quartz probe; and (6) fiber sample.

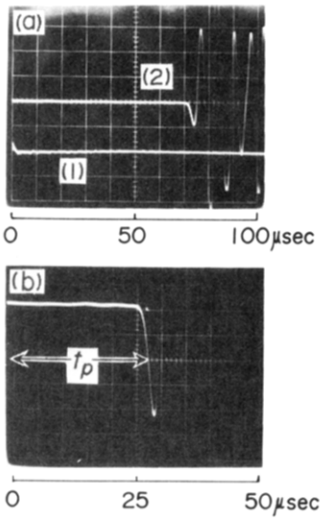

Figure 2. Pulse signals monitored with oscilloscope: (a) incident electric pulse (1) of a step function starting at t = 0 and received sonic pulse (2) in the form of modulated sine wave, x axis 10 μs/div, y axis arbitary; (b) received pulse with the time delay in the quartz probes eliminated by a trigger circuit.

are 1.483 g/cm^3 for PBA and 1.485 g/cm^3 for PPTA at room temperature (293 K).

TG Measurements. A Shimazu Model TG-20 thermogravimetric balance was used with a Type 20 cell. A fabric sample (ca. 10 mg) was heated at a nominal rate of 15 K/min in nitrogen stream.

TMA Measurements. Figure 1 is a schematic diagram of the measuring system developed by us. The measurements were done with heating and cooling rates of ±7.5 K/min in nitrogen stream under a constant load F. A bundle of the filament was used as a sample, which has a total cross section S ((3–7) × 10^{-3} cm^2) and a length L between two probes (about 17 cm). S was calculated from the mass, length, and density of the sample. The applied tensile stress σ equals F/S. The thermal strain ϵ equals $\Delta L/L$, where the displacement of the lower probe ΔL was detected by a linear variable differential transformer (LVDT). The temperature of the sample T was measured by a CA-thermocouple positioned near the center of the sample. The TMA-curve (ϵ vs. T) was recorded directly on an X–Y recorder.

Ultrasonic Measurements. The system shown in Figure 1 was used also for this purpose, and the temperature dependences of the sonic compliance and attenuation constant were obtained at the same time with a TMA measurement. Starting from the oscillating probe, the sonic pulse signal propagates through the distance L of the fiber sample and arrives at the receiving probe. Figure 2 shows the incident electric pulse of a step function and the received sonic pulse monitored by an oscilloscope. The received pulse has the shape of a modulated sine wave whose frequency is about 1 MHz. This shape and frequency mainly reflect the characteristic vibrational property of the oscillating transducer bonded to the quartz probe. The propagation time of the sonic wave in the probes can be estimated by contacting directly the two probes and eliminated from the total propagation time by a trigger circuit. In this way the propagation time t_p in the sample and the height h of the recieved signal were recorded. The sound velocity V and the sonic compliance J_s were calculated as

$$V = L/t_p \quad (1)$$

$$J_s = 1/(\rho V^2) \quad (2)$$

Here the length L and the density ρ at room temperature were used instead of those at each measuring temperature. As shown below, the change in L is a negligible order of 10^{-3} for the temperature shift of 300 K. Then the use of room temperature value L is approximately valid in eq 1. In such an approximation of constant L, the change in the factor $1/\rho$ in eq 2 is proportional to the change in the cross section S if the sample weight W does not change ($1/\rho = SL/W \propto S$). At the higher temperature (600 K or so), the change in S becomes of an order of 10$^{-1.5}$ as estimated by the X-ray method for PBA and PPTA.[35,36] This is rather unnegligible change. However, in the calculation of J_s in eq 2, we use the value of ρ at room temperature throughout this study. Therefore, J_s defined in this way denotes the compliance corresponding to the original cross section at room temperature and is proportional to the compliance per one molecular chain, irrespective of measuring temperature.

The incident pulse is attenuated during the propagation in the sample by a factor exp(−αL), where α is an attenuation constant of sound wave. Simple algebra gives the approximate relation $\alpha = \omega \tan \delta/(2V)$, where ω denotes the angular frequency, tan δ is the loss tangent of the complex compliance, and tan $\delta \ll 1$ is assumed. Employing the typical values of $\omega = 2\pi \times 10^6$ s^{-1} and $V = 10^6$ cm/s for our system, we obtain $\omega/(2V) \approx 3$ cm^{-1}. We define ρ_p, V_p, and S_p as the density, the sound velocity, and the cross-sectional area of the oscillating and receiving probes, respectively. In our experimental system, the inequality $\rho_p S_p V_p \gg \rho S V$ holds satisfactorily, the pulse signal is almost reflected at the boundaries between the probes and the sample, and the peak height of the received signal is expressed approximately by

$$h = h_o \exp(-\alpha L)\left(\frac{4\rho S V}{\rho_p S_p V_p}\right) \quad (3)$$

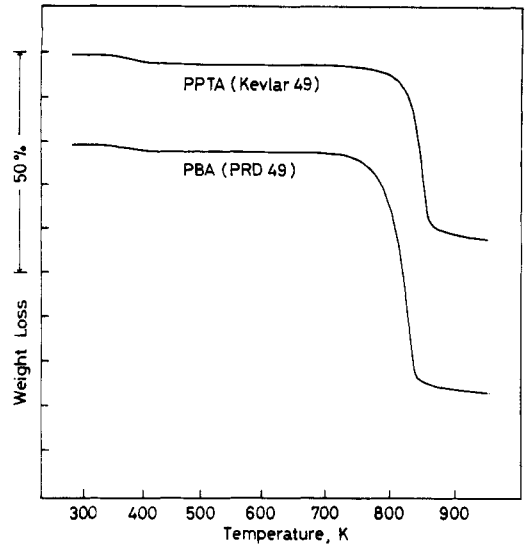

Figure 3. TG curves for PBA (PRD 49) and PPTA (Kevlar 49). The samples were washed with chloroform, dried in open air for 3 h, and tested in nitrogen gas stream with the rate dT/dt = 15 K/min.

where h_0 is the peak height of the pulse in the oscillating probe. Equation 3 is rewritten as

$$\alpha = \frac{1}{L}\log\left(\frac{V}{h}\right) + \frac{1}{L}\log\left(\frac{4\rho S h_0}{\rho_p S_p V_p}\right) \quad (4)$$

It is experimentally found that mainly the variables h and V are dependent on the measuring temperature and the second term of eq 4 can be assumed approximately constant. Then we employ here a relative attenuation constant Λ defined as

$$\Lambda = \frac{1}{L}\log\left(\frac{V}{h}\right) \quad (5)$$

Results and Discussion

Dehydration and Thermal Degradation. The results of TG measurement are shown in Figure 3 for PBA (PRD 49) and PPTA (Kevlar 49). The TG measurement for PPTA has been already reported by some previous workers,[35,37] while few TG results have been presented for PBA. We have measured the TG curves of both polymers and compared their thermal behaviors with one another. In the temperature range 320–410 K, both fibers lose a few percent of their weights. This phenomenon has been ascribed to the loss of absorbed water for PPTA,[37] especially in the noncrystalline part.[35] At higher temperatures, PBA and PPTA show almost no weight loss until 750 and 780 K and decrease rapidly in their weights around 820 and 850 K, respectively. This weight loss has been attributed to thermal degradation for PPTA.[35,37] Taking into account the similarity in the chemical structure of the two polymers and the TG results, we may say that the dehydration and degradation occur alos for PBA. The rate of degradation becomes slower at higher temperature, for example, at 920 K. At this temperature, the residual weight is 45% for PBA and 60% fo PPTA. Judging from the degradation temperature range and the residual weight, the thermal stability of PPTA is higher than that of PBA. At any rate, we may consider that the fibers are almost chemically stable in the range below 750 K. Therefore the TMA measurements and ultrasonic measurements were performed mainly in this temperature range as described below.

TMA Behavior. Figures 4–6 show TMA curves for PRD 49, Kevlar 49, and fiber B, respectively. In Figures 4 and 5, the measurements were performed under three

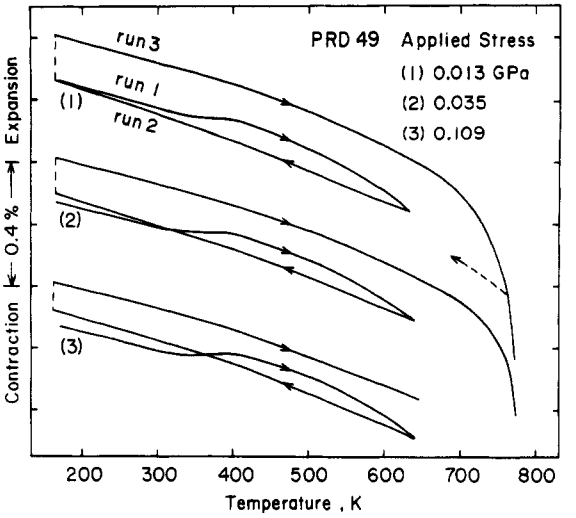

Figure 4. TMA curves for PRD 49 under various stresses. dT/dt = ca. ±7.5 K/min. The dashed line illustrates a conscious manual pen shift. The dashed arrow shows the behavior in the case of rapid cooling from the point noted.

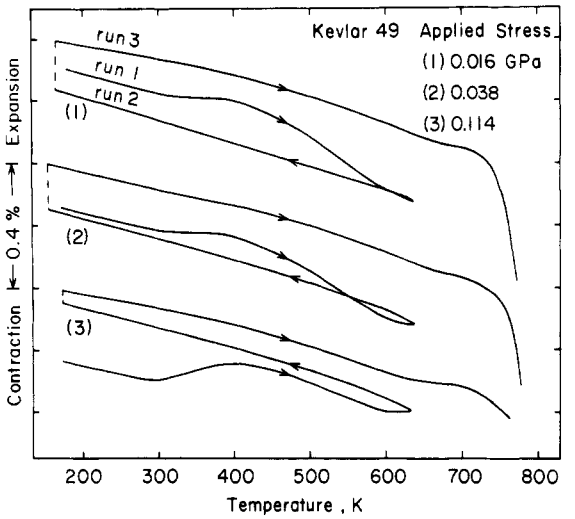

Figure 5. TMA curves for Kevlar 49 under various stresses. dT/dt = ca. ±7.5 K/min. The dashed line illustrates a conscious manual pen shift.

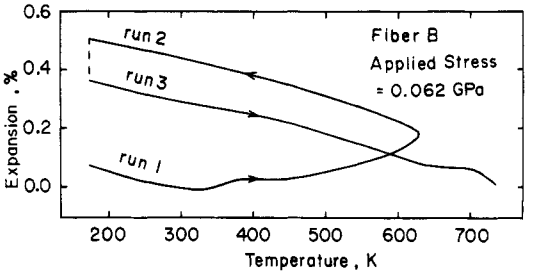

Figure 6. TMA curve for fiber B. σ = 0.062 GPa, and dT/dt = ca. ±7.5 K/min. The dashed line illustrates a conscious manual pen shift.

different stresses with an aim to clarify the effects of applied stress. All the measurements were performed in the course of heating (run 1; 170–630 K), cooling (run 2; 630–170 K), and second heating (run 3; 170 K through temperature at break) in order to compare the thermal behaviors of *annealed* and *as-received* samples. Here we regard a combined curve of run 1 and the part of run 3 higher than 630 K as the behavior of the as-received sample and that of run 2 and the part of run 3 lower than 630 K as the behavior of the annealed sample because annealing is attained during the first heating process up to

630 K. As seen in these figures, the TMA curves of runs 2 and 3 corresponding to the annealed state show a smooth and almost reversible thermal contraction (the negative slope), while the curves of run 1 deviate to some extent from these smooth curves. In this section, we will discuss first the TMA behaviors of as-received samples mainly by focusing our attention on the deviation from the smooth curve of runs 2 and 3.

A. Behaviors of As-Recevied Samples. As shown in Figures 4–6, an occurrence of irreversible elongation is commonly observed around 360 K in run 1. This elongation is about 0.07% and independent of the applied stress for PRD 49, while for Kevlar 49 it falls in the range 0.05–0.2% depending on the applied stress. For fiber B it is about 0.05%. The elongation occurs in parallel with the dehydration process (Figure 3), and so it might be interpreted by an increase of chain orientation in the noncrystalline part induced by the externally applied tensile force during the dehydration process. This parallel relationship has been already pointed out in the case of PPTA (Kevlar 49) by Brown and Ennis.[37]

In the temperature range 400–700 K, the three types of as-received samples exhibit the characteristic and mutually different TMA curves. In the range 400–630 K of run 1 in Figure 4, PRD 49 shows irreversible contraction, and the slope is almost independent of the applied stress. In Figure 6, fiber B shows a considerable and irreversible elongation, not contraction, in the range 430–600 K. This second elongation is observed above 600 K for Kevlar 49 in a curve inflection in run 1 in Figure 5. Such an elongational tendency is recognizable also in run 3 (630–700 K) in this figure. Some difference in the inflection temperature between two fibers, 430 K for fiber B and 600 K for Kevlar 49, might originate from the difference in such histories as spinning and heat treatment and thus in their resultant morphologies. Pottick et al.[38] have also pointed out such a difference in thermomechanical properties caused by the heat treatment between two PPTA fibers (Kevlar 49 and Kevlar 29 produced by Du Pont). Their arguments are essentially consistent with ours.

Above 700 K in run 3, the contraction curve becomes steeper for these three samples, especially under smaller stresses. When cooled rapidly from this temperature region, the fiber length does not recover the original value of run 3, as illustrated by a broken arrow in Figure 4.

B. Behaviors of Annealed Samples. Different from the case of as-received samples, the annealed samples show smooth and almost reversible contraction (runs 2 and 3 in Figures 4–6). The thermal expansion coefficients can be estimated from the slopes in the range 170–630 K as $(-7 \text{ to } -11) \times 10^{-6}$ K^{-1} for PRD 49 and $(-6 \text{ to } -9) \times 10^{-6}$ K^{-1} for Kevlar 49 and fiber B. These thermal expansion coefficients are markedly different in their sign and magnitude from those of isotropic or randomly oriented polymer solids (roughly estimated as $(5–20) \times 10^{-5}$ K^{-1})[32] and similar to the negative coefficient along the chain axis of lattice observed for many crystalline polymers[39–41] by X-ray diffraction (for example, the value for the c axis of polyethylene is ca. -1.1×10^{-5} K^{-1}).[40,41]

The above-mentioned thermal contraction of the chain axis originates from the lateral fluctuation of the molecular chain around the equilibrium position due to the thermal motion perpendicular to the chain axis.[40,41] Taking into account the paracrystalline structure of the present aramide fibers, we may ascribe the smooth and reversible contractions observed for the annealed samples mainly to this thermal contraction mechanism of the chain axis. In fact, we have confirmed experimentally that the contraction along the c axis of crystal lattice is just comparable with that of the bulk for PBA and PPTA fibers.[36] Such an idea of thermal fluctuation has also been found efficient to explain the temperature and stress dependences of the bulk compliance for PBA and PPTA fibers, as described in the next section.

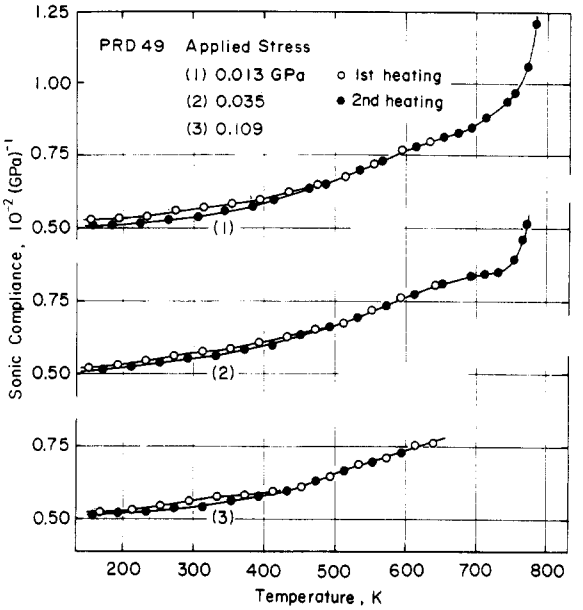

Figure 7. Temperature dependences of sonic compliance for PRD 49 under various stresses. dT/dt = ca. 7.5 K/min. Only the heating process is shown here.

In the case of flexible chain polymers, such as polyethylene, the macroscopic thermal expansion coefficient has been interpreted in terms of the combination effects of the thermal contraction in the crystalline part, the thermal expansion in the amorphous part, and the rubber-elastic effect of prestretch tie molecule.[32] We can say that the situation for the flexible chain polymers is somewhat complicated compared with that of aramide fibers.

Sonic Compliance and Attenuation Constant. In Tables I and II are compared our typical data of moduli at room temperature with those obtained by other investigators for PBA and PPTA. For polymer materials the macroscopic modulus depends strongly on the production condition or the morphology of the sample. The values of sonic modulus for PRD 49 are comparable to the lattice or theoretical modulus for PBA (Table I). The values of sonic modulus for Kevlar 49 and fiber B reach 1 and $^1/_3$ of the lattice or theoretical moduli for PPTA, respectively (Table II). These values also support their highly oriented paracrystalline structure.

In Figures 7–9 the temperature dependences of sonic compliance for PRD 49, Kevlar 49, and fiber B are shown, respectively. They were obtained in parallel with the TMA curves shown in Figures 4–6. In Figure 10 are shown typical temperature dependences of the attenuation constant Λ for PRD 49 and Kevlar 49, which were measured simultaneously with sonic compliances in Figures 7(2) and 8(3). In these figures, the open and filled circles represent the data on the the first (run 1) and second (run 3) heating processes, respectively. As in the TMA measurements, the data of run 2 (cooling process) were essentially similar to those of run 3, suggesting a reversibility in mechanical properties after the annealing treatment. Therefore, the curve of run 2 is not presented in these figures.

A. Behaviors of As-Received Samples. In the temperature range up to 400 K, the attenuation constant Λ

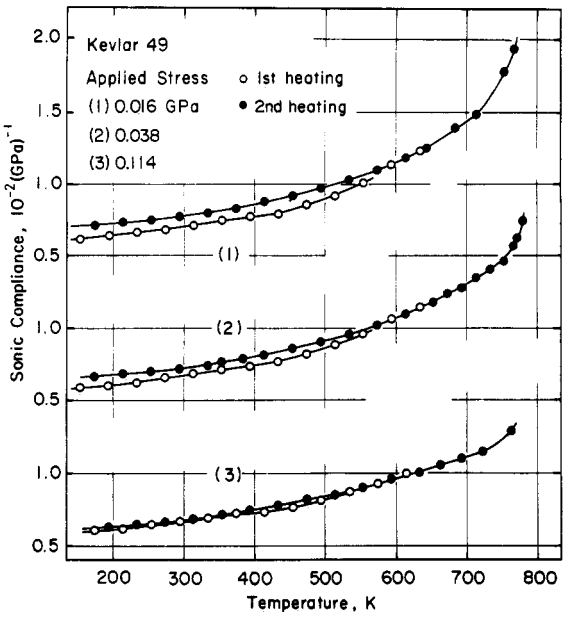

Figure 8. Temperature dependences of sonic compliance for Kevlar 49 under various stresses. dT/dt = ca. 7.5 K/min. Only the heating process is shown here.

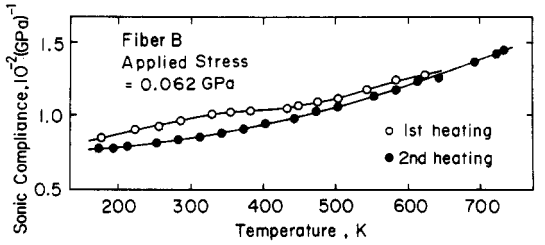

Figure 9. Temperature dependence of sonic compliance for fiber B. σ = 0.062 GPa, and dT/dt = ca. 7.5 K/min. Only the heating process is shown here.

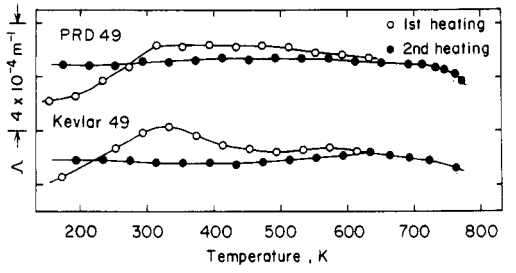

Figure 10. Temperature dependences of sound attenuation constant Λ for PRD 49 (σ = 0.035 GPa) and Kevlar 49 (σ = 0.114 GPa). dT/dt = ca. 7.5 K/min. Only the heating process is shown here.

shows some peaks (open circles in Figure 10), although the broadness of peak changes from sample to sample.

On the basis of broad-line NMR and dynamic viscoelastic measurements, such a peak for PPTA has been attributed to the β relaxation or some molecular motion in the noncrystalline part.[35,42] In the same temperature region, the sonic compliance reveals some transient slowing down of the slope (open circles in Figures 7–9): 350–380 K for PRD 49, around 400 K for Kevlar 49, and 350–430 K for fiber B. This slowing down appears inconsistent with the above-mentioned observation of Λ peak, because in usual cases the compliance increases in the relaxation region. However, when the results of TG and TMA discussed in the previous sections are taken into account, such an apparent inconsistency can be reasonably interpreted as follows.

The observed phenomena in this range may be summarized for Kevlar 49 as (1) the peak of Λ appearing around 320 K (Figure 10), (2) the dehydration process in the range 340–405 K (Figure 3), (3) the dimensional increase in the range 360–400 K (Figure 5), and (4) the slowing down of the increasing tendency in sonic compliance around 400 K (Figure 8). Experimental results 1 and 2 suggest that some molecular motions might occur in the hydrated noncrystalline part which induce the relaxational phenomenon detectable as a peak of Λ. Due to such a molecular motion followed by the dehydration process, a slight increase in chain orientation in the noncrystalline region occurs under the application of tensile stress, and it is recognized as the dimensional increase (3) and as the resultant slowing down of the increasing tendency in compliance (4). This mechanism can be applied also to the cases of PRD 49 and fiber B.

In the temperature range 430–630 K, the sonic compliance increases monotonously. But the values for Kevlar 49 and fiber B change slightly between the first and second heating processes. Such a change in compliance is found to be dependent on the applied stress and consistent with the stress dependence of the thermal contraction or expansion along the fiber direction (Figure 5). Above 730 K, the slope of the compliance against temperature becomes steeper for PRD 49 and Kevlar 49, corresponding well to the irreversible contractions above 700 K (Figure 4 and 5). The values of Λ decrease even in this temperature range.

B. Behaviors of Annealed Samples. The temperature dependences of sonic compliance and Λ for annealed samples (filled circles) are rather monotonous compared with those for the as-received samples (open circles) in Figures 7–10. In particular, it is noteworthy that no obvious dispersion peak of Λ is observed for the annealed states (Figure 10). As temperature rises, the compliance for annealed states increases gradually and their slopes become steeper (Figures 7–9). These increases are estimated as about 50% for PRD 49 and about 70% for Kevlar 49 and fiber B in the range 170–630 K. In the TMA curves (Figures 4–6), we have observed the reversible contraction of fiber length for annealed samples and ascribed it to the thermally fluctuated molecular motion perpendicular to the chain axis. It may be natural to consider that the contracted chain at a certain temperature has a compliance greater than that of the fully extended chain at absolute zero temperature. This is the reason why the sonic compliances of these fibers increase monotonously with a rise of temperature. We should expect this type of temperature dependence of compliance to be detected also for the crystal lattice, the experimental results being reported in a following paper.[43]

At a temperature range of 400–630 K, some decrease in compliance is recognized with an increase of the applied stress (from 1 to 3 in Figures 7 and 8). As shown in Figure 11, the stress dependence of compliance was measured at several fixed temperatures for annealed PRD 49 and Kevlar 49. These measurements were performed under cyclic loading and unloading conditions, and the reversible stress dependence of sonic compliance has been confirmed for both fibers. This stress dependence is negative; $\partial J_s/\partial\sigma < 0$. Figure 12 shows the temperature dependence of $\partial J_s/\partial\sigma$ for PRD 49 and Kevlar 49. The negative sign and temperature dependence of $\partial J_s/\partial\sigma$ might be also interpreted qualitatively as follows, in terms of the aforementioned thermal fluctuation.

When the tensile stress acts on the thermally fluctuated molecular chain, the degree of chain contraction due to the

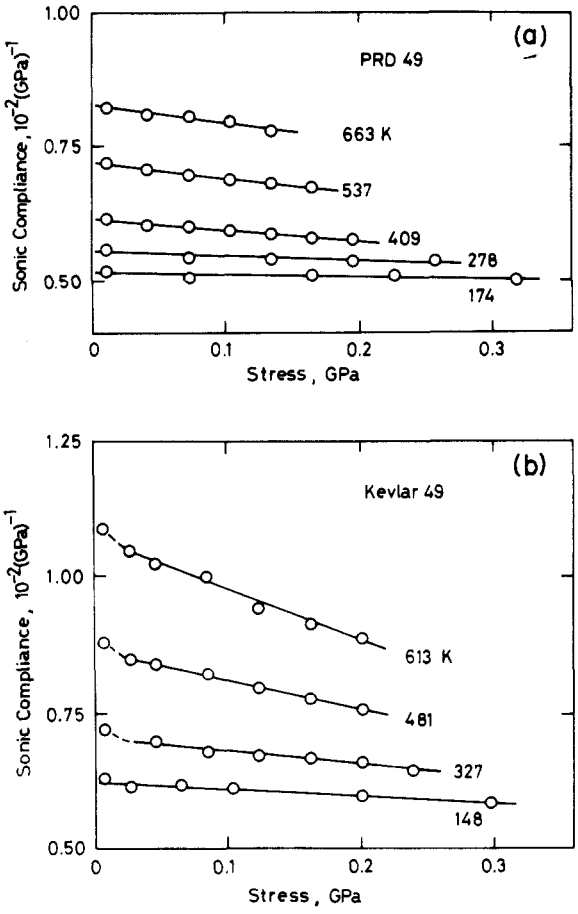

Figure 11. Stress dependences of sonic compliance at the various temperatures measured for (a) PRD 49 (annealed at 663 K for 30 min) and (b) Kevlar 49 (annealed at 613 K for 30 min).

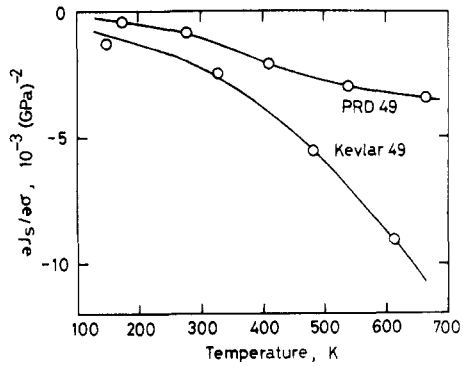

Figure 12. Temperature dependences of $\partial J_s/\partial\sigma$ for PRD 49 and Kevlar 49, where J_s and σ denote sonic compliance and tensile stress, respectively.

fluctuation will be diminished in comparison with that expected under no stress. The compliance will be smaller under a finite stress. This is the reason why $\partial J_s/\partial\sigma < 0$. The magnitude of decrease in compliance under tensile stress will depend on how much the chain contracts, and the chain contracts more highly at higher temperature by the thermal agitation. Then the value of $-\partial J_s/\partial\sigma$ will become larger with a rise of temperature. This is the reason why $\partial^2 J_s/\partial T\partial\sigma < 0$ (T denotes temperature).

If the static strain ϵ is expressed as a function of T and σ under a suitable model including a thermal fluctuation mechanism, the temperature dependence of J_s and $\partial J_s/\partial\sigma$ may be derived consistently and quantitatively. The theoretical investigation of this subject is now in process.

Registry No. PBA (SRU), 24991-08-0; PBA (hompolymer), 25136-77-0; PPTA (SRU), 24938-64-5; PPTA (copolymer), 25035-37-4.

References and Notes

(1) Morgan, P. W. *Macromolecules* **1977**, *10*, 1831.
(2) Kwolek, S. L.; Morgan, P. W.; Schaefgen, J. R.; Gulrich, L. W. *Macromolecules* **1977**, *10*, 1390.
(3) Kwolek, S. L. U.S. Patent 3 600 350, Aug 17, 1971.
(4) Kwolek, S. L. U.S. Patent 3 671 542, June 20, 1972.
(5) Blade, H. U.S. Patent 3 767 756, Oct 23, 1973.
(6) Bair, T. I. U.S. Patent 3 817 941, June 18, 1974.
(7) Tashiro, K.; Kobayashi, M.; Tadokoro, H. *Macromolecules* **1977**, *10*, 413.
(8) Hummel, J. P.; Flory, P. J. *Macromolecules* **1980**, *13*, 479.
(9) Arpin, M.; Strazielle, C. *Makromol. Chem.* **1976**, 581.
(10) Alfonso, G. C.; Bianchi, E.; Cifferi, A.; Russo, S.; Varenti, B. *J. Polym. Sci., Polym. Symp. No. 65*, 213.
(11) Wong, C. P.; Ohnuma, H.; Berry, G. C. *J. Polym. Sci., Polym. Symp.* **1978**, *No. 65*, 173.
(12) Tsvetkov, V. N.; Andreeva, L. N. *Adv. Polym. Sci.* **1978**, *39*, 95–207.
(13) Bair, T. I.; Morgan, P. W.; Killian, F. L. *Macromolecules* **1977**, *10*, 1396.
(14) Panar, M.; Beste, L. F. *Macromolecules* **1977**, *10*, 1401.
(15) Papkov, S. P.; Kulichikhin, V. G.; Kalmykova, V. D. *J. Polym. Sci., Polym. Phys. Ed.* **1974**, *12*, 1753.
(16) Hasegawa, R. K.; Chatani, Y.; Tadokoro, H. *Meeting of the Crystallogrpahic Society of Japan*, Osaka, Japan, 1973; Preprint, p 21.
(17) Northolt, M. G.; Van Aartsen, J. J. *J. Polym. Sci., Polym. Lett. Ed.* **19738**, *11*, 333.
(18) Yabuki, K.; Ito, H.; Ota, T. *Sen'i Gakkaishi* **1975**, *31*, T-524.
(19) Williams, A. D.; Flory, P. J. *J. Polym. Sci., Polym. Phys. Ed.* **1967**, *5*, 417.
(20) Yabuki, K.; Ito, H.; Ota, T. *Sen'i Gakkaishi* **1976**, *32*, T-55.
(21) Yabuki, K.; Koda, H.; Endo, S.; Kajima, I.; Yukimatsu, K.; Konomi, T. *Sen'i Gakkaishi* **1978**, *34*, T-342.
(22) Northolt, M. G.; Van Aartsen, J. J. *J. Polym. Sci., Polym. Symp.* **1977**, *No. 58*, 283.
(23) Kaji, K.; Sakurada, I. *Meeting of the Society of Polymer Science*, Kobe, Japan, 1975; p 56.
(24) Gaymans, R. G.; Tijssen, J.; Harkama, S.; Bantjes, A. *Polymer* **1976**, *17*, 517.
(25) Slutsker, L. I.; Utevskii, L. E.; Chereiskii, Z. Yu.; Perepelkin, K. E. *J. Polym. Sci., Polym. Symp.* **1977**, *No. 58*, 339.
(26) Fielding-Russell, G. S. *Text. Res. J.* **1971**, *41*, 860.
(27) Slutsker, L. I.; Utevskii, L. E.; Chereiskii, Z. Yu.; Perepelkin, K. E. *J. Polym. Sci., Polym. Symp.* **1977**, *No. 58*, 339. Perepelkin, K. E.; Chereiskii, Z. Yu. *Prepr. Int. Symp. Man-Made Fibers, Kalinin, USSR* **1974**, *1*, 142.
(28) Tashiro, K.; Kobayashi, M.; Tadokoro, H. *Macromolecules* **1977**, *10*, 413.
(29) Takayanagi, M.; Imada, K.; Kajiyama, T. *J. Polym. Sci., Part C* **1966**, *15*, 263.
(30) Sakurada, I.; Kaji, K. *J. Polym. Sci. Part C* **1970**, *31*, 57.
(31) Holliday, L.; White, J. W. *Pure* Appl. *Chem.* **1971**, *26*, 545.
(32) Choy, C. L.; Chen, F. C.; Young, K. *J. Polym. Sci., Polym. Phys. Ed.* **1981**, *19*, 335.
(33) Du Pont, "Kevlar Aramide Data Manual", 1975.
(34) Tashiro, K.; Kobayashi, M., to be published.
(35) Haraguchi, K.; Kajiyama, T.; Takayanagi, M. *Sen'i Gakkaishi* **1977**, *33*, T-535.
(36) Ii, T.; Tashiro, K.; Kobayashi, M.; Tadokoro, H., to be published.
(37) Brown, J. R.; Ennis, B. C. *Text. Res. J.* **1977**, *47*, 62.
(38) Pottick, L. A.; Allen, S. R.; Farris, R. J. *J. Appl. Polym. Sci.* **1984**, *29*, 3915.
(39) Wakelin, J. H.; Sutherland, A.; Beck, Jr., L. R. *J. Polym. Sci.* **1960**, *42*, 139.
(40) Davis, G. T.; Ebby, R. K.; Colson, J. P. *J. Appl. Phys.* **1970**, *37*, 4316.
(41) Kobayashi, Y.; Keller, A. *Polymer* **1970**, *11*, 114.
(42) Frosini, V.; Levita, G.; Butta, E. *Polym. Eng. Sci.* **1979**, *19*, 56.
(43) Ii, T.; Tashiro, K.; Kobayashi, M.; Tadokoro, H., to be published.